



## NRC Publications Archive Archives des publications du CNRC

**High extinction ratio and broadband silicon TE-pass polarizer using subwavelength grating index engineering**  
Xiong, Yule; Xu, Dan-Xia; Schmid, Jens H.; Cheben, Pavel; Ye, Winnie N.

This publication could be one of several versions: author's original, accepted manuscript or the publisher's version. / La version de cette publication peut être l'une des suivantes : la version prépublication de l'auteur, la version acceptée du manuscrit ou la version de l'éditeur.  
For the publisher's version, please access the DOI link below. / Pour consulter la version de l'éditeur, utilisez le lien DOI ci-dessous.

**Publisher's version / Version de l'éditeur:**

<https://doi.org/10.1109/JPHOT.2015.2483204>  
*IEEE Photonics Journal*, 2015-10-01

**NRC Publications Record / Notice d'Archives des publications de CNRC:**

<https://nrc-publications.canada.ca/eng/view/object/?id=dc22c28e-4d99-439d-a176-076389f9bf5b>  
<https://publications-cnrc.canada.ca/fra/voir/objet/?id=dc22c28e-4d99-439d-a176-076389f9bf5b>

Access and use of this website and the material on it are subject to the Terms and Conditions set forth at  
<https://nrc-publications.canada.ca/eng/copyright>  
READ THESE TERMS AND CONDITIONS CAREFULLY BEFORE USING THIS WEBSITE.

L'accès à ce site Web et l'utilisation de son contenu sont assujettis aux conditions présentées dans le site  
<https://publications-cnrc.canada.ca/fra/droits>  
LISEZ CES CONDITIONS ATTENTIVEMENT AVANT D'UTILISER CE SITE WEB.

**Questions?** Contact the NRC Publications Archive team at  
PublicationsArchive-ArchivesPublications@nrc-cnrc.gc.ca. If you wish to email the authors directly, please see the first page of the publication for their contact information.

**Vous avez des questions?** Nous pouvons vous aider. Pour communiquer directement avec un auteur, consultez la première page de la revue dans laquelle son article a été publié afin de trouver ses coordonnées. Si vous n'arrivez pas à les repérer, communiquez avec nous à PublicationsArchive-ArchivesPublications@nrc-cnrc.gc.ca.



# High extinction ratio and broadband silicon TE-pass polarizer using subwavelength grating index engineering

Yule Xiong,<sup>1,2</sup> Dan-Xia Xu,<sup>1</sup> Jens H. Schmid,<sup>1</sup> Pavel Cheben,<sup>1</sup> and Winnie N. Ye <sup>2</sup>

<sup>1</sup>Information and Communications Technologies, National Research Council Canada, Canada

<sup>2</sup>Department of Electronics, Carleton University, Ottawa, Canada K1S 5B6

**Abstract:** We propose and experimentally demonstrate a novel approach to implement a low loss, broadband and compact transverse electric (TE)-pass polarizer on a silicon-on-insulator (SOI) platform. The TE-polarizer utilizes a subwavelength grating (SWG) structure to engineer the waveguide equivalent material index. In this work, the SWG-based polarizer only supports its fundamental TE mode while the transverse magnetic (TM) mode is suppressed under the cut-off condition, i.e., the TM mode leaks from the waveguide with a low reflection. The simulations predict that the bandwidth to achieve a polarization extinction ratio (ER) of 35 dB exceeds 200 nm. Experimentally, the measured polarization ER is ~30 dB and the average insertion loss is 0.4 dB, in the wavelength range 1470 nm - 1580 nm. The fabricated TE-polarizer has a compact length of 60  $\mu\text{m}$ .

**Index Terms:** waveguides, subwavelength structures, silicon nanophotonics.

## 1. Introduction

Polarization management is an important research topic in silicon photonics [1]. High refractive index contrast makes silicon waveguides highly polarization dependent. To address this issue, various types of passive polarization management components have been reported recently, including polarization splitters [2, 3], rotators [4-10] and polarizers [11-16]. Among them, polarizers which simply filter the undesired polarization state are suitable for many applications. Silicon hybrid plasmonic waveguide polarizers [11, 12] have recently attracted significant attention because of their small footprint and broadband operation. However, such devices generally have a comparatively large excess loss and the fabrication process involving metals restricts their applications. Polarizers based on photonic-crystal (PhC) structures are also typically lossy and sensitive to fabrication errors [13]. On the other hand, a waveguide polarizer with partially etched waveguides is easier to fabricate, but it tends to be a long structure, on the order of 1 mm [14]. In ref. [15], a TM-pass polarizer was designed by limiting the width (between 180 and 250 nm) of a wire waveguide with a Si thickness of 300 nm. Only the TM fundamental mode is supported in this specific geometry, while the fundamental TE-mode is suppressed by the cut-off condition. However, to implement this concept as a TE-pass polarizer, the Si layer thickness of less than 200 nm is required, not compatible with 220 nm SOI typically used in silicon photonics foundries since waveguide height is set by the silicon layer thickness of the substrate and local etching to change the thickness complicates the fabrication process. In such designs that rely on pure geometry manipulation, the waveguide parameters are inflexible, hence limiting the implementation to practical applications.

Recently, the subwavelength grating (SWG) effect has been shown to provide new degrees of freedom for implementing advanced silicon photonic components [17]. The SWG comprises materials with different refractive indices arrayed at a pitch which is substantially smaller than the wavelength of light propagating in the structure, therefore behaving effectively as an equivalent homogenous medium [17-20]. The equivalent material index of the SWG can be modified by simply changing the grating duty ratio [17]. A TM-pass polarizer was realized in [16] using the SWG effect. However, the structure acts as a Bragg reflector for the incident TE-polarized light, which limits its usability, particularly when operating with laser diodes which are sensitive to back reflections.

Here we propose a general strategy to circumvent these limitations of the previous waveguide polarizer designs. Specifically, we demonstrate the first SWG engineered TE-pass polarizer in silicon waveguides. The refractive index synthesis by the SWG is used in conjunction with judicious selection of the waveguide parameters to adjust the mode cut-off condition of the waveguide, yielding a low-loss and broadband TE-pass polarizer. Our SWG design has a large flexibility in the selection of the waveguide parameters because the mode effective index can be controlled by the SWG effect.

## 2. Polarizer Design

The proposed TE-pass polarizer is implemented as a SWG waveguide in 220 nm SOI, as it is schematically shown in Figs. 1(a) and 1(b). The main structural parameters are: the waveguide width  $W$  and height  $H$ , the grating pitch  $\Lambda$ , and the polarizer length  $L$ . The SWG waveguide comprises alternating media with high (silicon) and low (air) refractive indices, with a period  $\Lambda$  along the light propagation direction. The silicon segment length is denoted as  $a$ , i.e. the grating duty ratio is  $\eta = a/\Lambda$ . SWG-wire tapered transitions with a length  $L_t$  are used to couple the light between the SWG waveguide and the input and output silicon wire waveguides [21]. In order to achieve the polarizer performance, vertically asymmetric waveguide geometry, i.e., the upper cladding has a different refractive index than the buried oxide (BOX) cladding layer, is necessary for achieving the cut-off condition for the TM mode. For simplicity, the upper cladding is air.

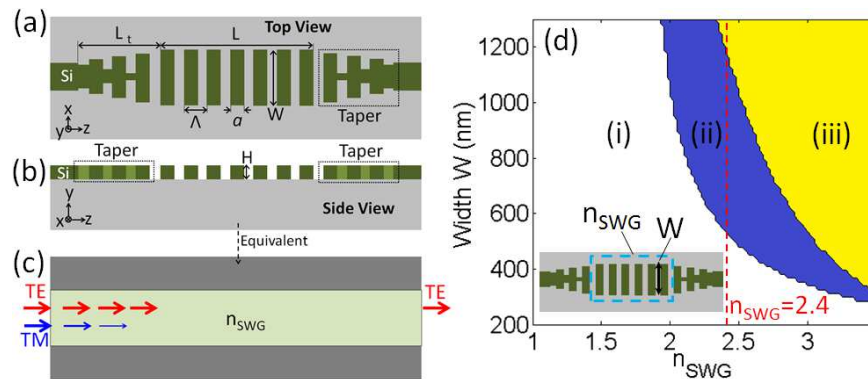


Fig. 1 Schematics of the TE-pass polarizer based on a subwavelength grating (SWG) waveguide. (a) Device top view; (b) cross-section (side view); (c) the SWG-polarizer represented as an equivalent wire waveguide with an engineered core refractive index  $n_{\text{SWG}}$ ; and (d) 3 regions of the cut-off conditions of the SWG waveguide as a function of the SWG waveguide width  $W$  and the index  $n_{\text{SWG}}$ , for Si layer thickness  $H=220$  nm: (i) the cut-off region with no guided mode supported; (ii) region supporting only the fundamental TE-like Bloch mode; (iii) region supporting both the fundamental TE- and TM-like Bloch modes.

We first evaluate the Bloch mode [17] cut-off condition of the SWG waveguide using the finite element method (FEM), by considering the SWG waveguide as an equivalent wire waveguide with an engineered core refractive index  $n_{\text{SWG}}$  [Fig. 1(c)]. The value of  $n_{\text{SWG}}$  can be controlled by selecting a specific duty ratio  $\eta = a/\Lambda$  [22]. We assume the following parameters: a free-space wavelength of  $\lambda_0=1550$  nm, the refractive index of air  $n_{\text{air}}=1$ , the refractive indices of silicon and the  $\text{SiO}_2$  of  $n_{\text{Si}}=3.476$  and  $n_{\text{SiO}_2}=1.444$ , respectively. The Bloch mode cut-off conditions determined by the index  $n_{\text{SWG}}$  and the waveguide width  $W$  can be observed in Fig. 1(d), for the waveguide height  $H=220$ nm, which is commonly used in silicon photonics foundries. When the engineered refractive index  $n_{\text{SWG}}$  increases from 1 (air) to 3.476 (silicon), the mode cut-off condition of the SWG waveguide changes from no supported propagating mode (region i), to supporting only the TE-like Bloch mode (region ii), and supporting both the TE- and TM-like Bloch modes (region iii). Figure 1(d) shows that the index engineering of  $n_{\text{SWG}}$  can be used to control the Bloch mode cut-off condition. By modifying  $n_{\text{SWG}}$ , a range of waveguide widths can be selected where the SWG waveguide can only support the TE Bloch mode [region ii in Fig. 1(d)], while the TM mode is cut-off and radiated primarily to the Si substrate through the BOX layer.

Next, the pitch and duty ratio of the SWG waveguide are set to  $\Lambda=300$  nm and  $\eta=0.5$ , respectively, which are the typical feature sizes that can be reliably fabricated. The length  $L_t$  of the SWG-wire

transitional taper is set to 5  $\mu\text{m}$ , for the optimal trade-off between the device size and the taper loss. We calculated the SWG-wire waveguide transition loss as 0.1 dB. As it was previously demonstrated [17], the theoretical loss limit for this type of tapers indeed is very low,  $\sim 0.04$  dB. Using the effective medium approximation in SOI waveguides [22], the engineered refractive index of the SWG waveguide  $n_{\text{SWG}}$  is 2.4 with a duty ratio of  $\eta=0.5$ . In our design, the grating pitch  $\Lambda$  is on the order of a few hundreds of nanometers, while the pitch deviations due to fabrication inaccuracies are no more than several nanometers. Consequently, the fabrication inaccuracies are not expected to affect the grating's subwavelength operation regime. Since the equivalent core refractive index of the SWG  $n_{\text{SWG}}$  is modified by changing the grating duty ratio  $\eta$ , the fabrication inaccuracies on the grating duty ratio  $\eta$  will change the engineered core refractive index  $n_{\text{SWG}}$ . However, as shown in Fig. 1(d), the polarizer can tolerate a relatively broad range of  $n_{\text{SWG}}$  in region (ii), specifically  $2 < n_{\text{SWG}} < 2.5$  if the waveguide width is  $W=1100$  nm. This corresponds to a duty ratio range of  $0.3 < \eta < 0.6$ , yielding a device which is substantially tolerant to the duty ratio deviations. According to Fig. 1(d), a TE-pass polarizer can be implemented using an SWG waveguide with width ranging from 550 nm to 1200 nm, therefore allowing a large fabrication tolerance to waveguide width variations.

The performance of the proposed TE-pass polarizer is evaluated using the three-dimensional finite-difference time-domain (3D-FDTD) simulations. The FDTD simulations include both the SWG-wire taper sections and the periodic SWG polarizer section. Figure 2 shows the simulated transmittance for the TE and TM modes for various SWG waveguide lengths ( $L$ ) and widths ( $W$ ), at the central wavelength of  $\lambda_0 = 1550$  nm. It is clear that the transmittance decreases with reducing the width  $W$  of the SWG waveguide. It can also be observed that the SWG length  $L$  has a negligible effect on the TE mode, while the TM mode attenuation substantially increases with  $L$ . In our nominal design, the width of the SWG waveguide is set to  $W=1100$  nm.

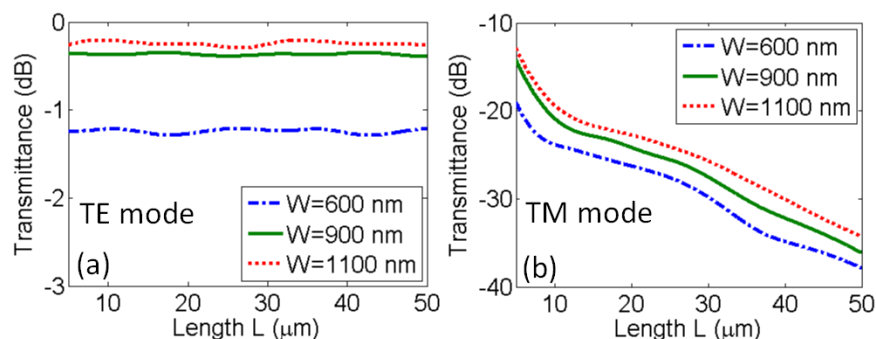


Fig. 2 Calculated transmittance of the TE-pass polarizer as a function of the SWG waveguide length  $L$  for different widths  $W$ .  $H=220$  nm,  $\Lambda = 300$  nm,  $\eta=0.5$ , and  $\lambda_0 = 1550$  nm. Calculated by the 3D-FDTD method with the grid size  $\Delta x=20$  nm,  $\Delta y=30$  nm and  $\Delta z=20$  nm and a time step  $\Delta t = 20$  ps.

Figure 3 shows the calculated transmission ( $T_{\text{TE}}$  and  $T_{\text{TM}}$ ) and reflection ( $R_{\text{TE}}$  and  $R_{\text{TM}}$ ) coefficients for the TE and TM input modes as a function of the SWG length  $L$ . Here, we define the transmission  $T$  and  $R$  as  $T=P_{\text{out}}/P_{\text{in}}$  and  $R=P_{\text{back}}/P_{\text{in}}$ , respectively.  $P_{\text{in}}$ ,  $P_{\text{out}}$  and  $P_{\text{back}}$  are the input, output and back-reflected mode power, respectively. The TE mode exhibits a low waveguide propagation loss, including the SWG-wire transition loss. On the other hand, the TM mode attenuates exponentially and leaks away from the waveguide core, primarily to the silicon substrate. The reflection coefficients for both the TE and TM polarizations are below  $-15$  dB and are not significantly affected by the SWG waveguide length  $L$ . For the waveguide width  $W=1100$  nm, the SWG length  $L$  of 10  $\mu\text{m}$  yields a polarization extinction ratio (ER) of 20 dB. In our device, the SWG waveguide length is chosen as  $L=50$   $\mu\text{m}$ , for a polarization extinction ratio ER of  $\sim 35$  dB.

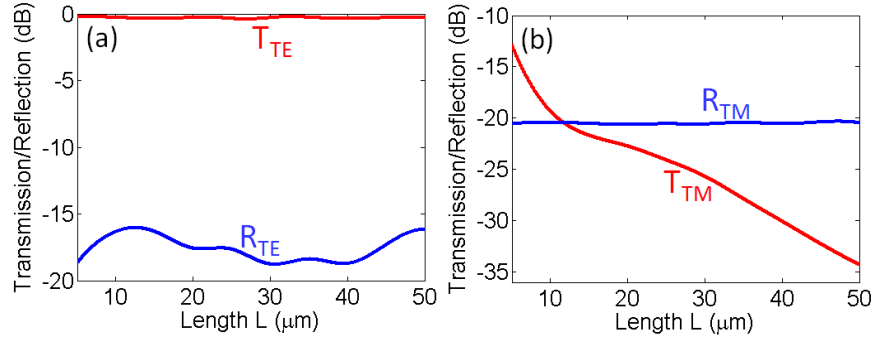


Fig. 3 The polarizer transmission and reflection coefficients as a function of the SWG waveguide length  $L$  for (a) TE-like mode ( $T_{TE}$  and  $R_{TE}$ ) and (b) TM-like mode ( $T_{TM}$  and  $R_{TM}$ ).  $W=1100$  nm,  $H=220$  nm,  $\Lambda = 300$  nm,  $\eta=0.5$ , and  $\lambda_0 = 1550$  nm. Calculated by the 3D-FDTD method with the grid size  $\Delta x=20$  nm,  $\Delta y=30$  nm and  $\Delta z=20$  nm and a time step  $\Delta t = 20$  ps.

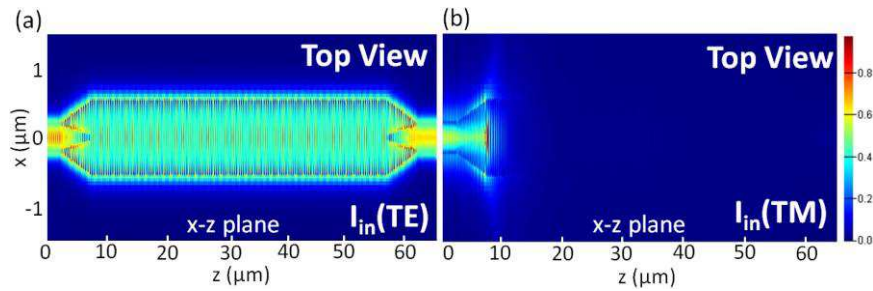


Fig. 4 Light field evolution ( $|E|$ ) along the TE-pass polarizer, as calculated by the 3D-FDTD method. Top view ( $x$ - $z$  plane), input is located at the left port. (a) TE input and (b) TM input.  $W = 1100$  nm,  $H = 220$  nm,  $L = 50$   $\mu\text{m}$ ,  $L_t = 5$   $\mu\text{m}$ ,  $\Lambda = 300$  nm,  $\eta = 0.5$ , and  $\lambda_0 = 1550$  nm.

Figures 4(a) and 4(b) show the light field evolution in the TE-pass polarizer for the wavelength of 1550 nm. It is observed that the TE polarized light propagates in the structure with a low loss, while the TM polarization is efficiently attenuated. Figure 5 shows the calculated transmission ( $T$ ) and reflection ( $R$ ) coefficients as a function of wavelength ( $\lambda$ ). The transmission coefficient for the TE polarization,  $T_{TE}(\lambda)$ , is about  $-0.3$  dB, while the TM polarization,  $T_{TM}(\lambda)$  is very low ( $< -35$  dB), in a broad wavelength range from 1450 nm to 1650 nm. The calculated reflection  $R$  for the TE and TM polarizations are  $< -16$  dB and  $< -20$  dB, respectively, at  $\lambda_0 = 1550$  nm. The transmission loss and the reflections are mainly attributed to the SWG-wire taper sections.

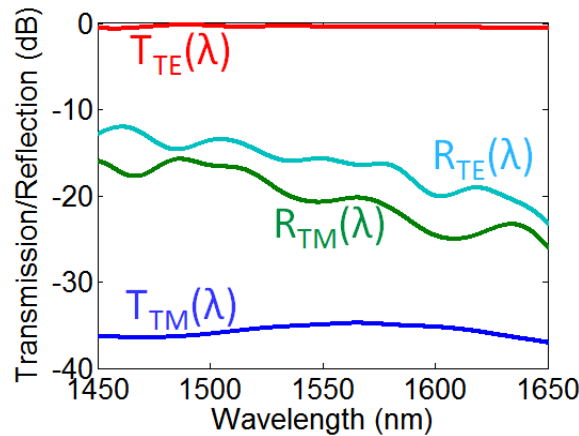


Fig. 5 Calculated wavelength dependence of polarizer transmission ( $T$ ) and reflection ( $R$ ) coefficients. Structural parameters:  $W = 1100$  nm,  $H = 220$  nm,  $L = 50\mu\text{m}$ ,  $L_t = 5$   $\mu\text{m}$ ,  $\Lambda = 300$  nm, and  $\eta = 0.5$ . Calculated by the 3D-FDTD method with the grid size  $\Delta x=20$  nm,  $\Delta y=30$  nm and  $\Delta z=20$  nm, and a time step  $\Delta t = 20$  ps.

### 3. Fabrication and Experimental Results

The polarizer was fabricated on a silicon-on-insulator substrate with a 220 nm silicon waveguide layer and a 2  $\mu\text{m}$  BOX layer. The e-beam lithography was used to pattern the polarizer structure and the interconnecting waveguides under an etch mask of a high-contrast hydrogen silsesquioxane (HSQ) resist. An inductively coupled plasma reactive ion etching (ICP-RIE) was used to transfer the waveguide layout onto the silicon layer. The total device length including the SWG ( $L=50 \mu\text{m}$ ) and the taper sections ( $2L_t=10 \mu\text{m}$ ) is 60  $\mu\text{m}$ . The images of the fabricated polarizer are shown in Fig. 6.

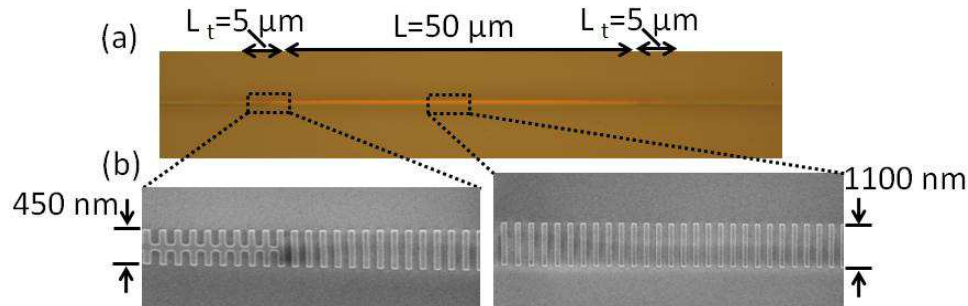


Fig. 6 (a) Optical microscope image of the fabricated polarizer; (b) SEM images of the transition taper section (left) and the periodic SWG polarizer section (right).

To experimentally characterize the polarizer performance, a tunable laser was coupled into the chip using a polarization maintaining lensed fiber with a Gaussian beam waist of  $\sim 3 \mu\text{m}$  and a polarization controller, as shown in Fig. 7(a). To determine the reflection coefficients, an optical fiber circulator was used at the input of the chip, as shown in Fig. 7(b).

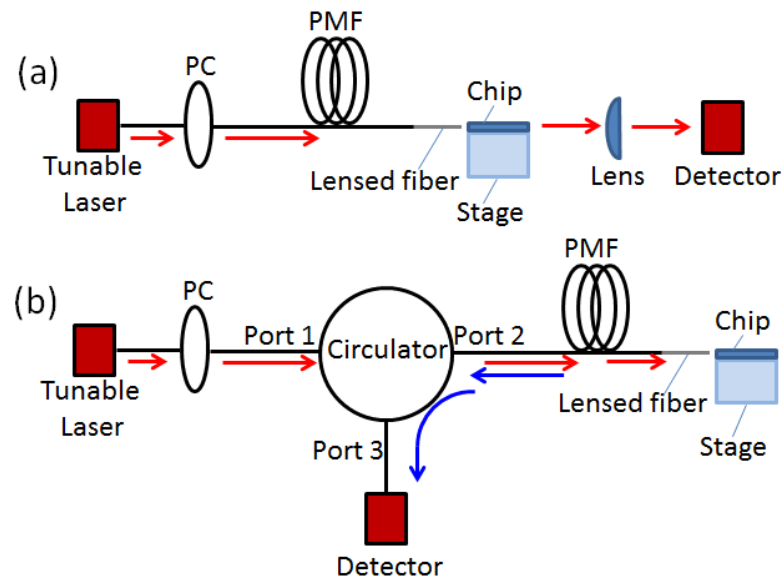


Fig. 7 Experimental setups for (a) transmission and (b) reflection measurements. PC: Polarization Controller, PMF: Polarization Maintaining Fiber.

Figure 8(a) shows the measured transmission coefficients for the TE and TM polarized inputs. The fiber-chip coupling loss and the measurement system loss were subtracted by using an independent loss measurement on a set of straight reference waveguides. The average loss for the TE mode is  $\sim 0.4 \text{ dB}$  and the polarization extinction ratio is  $\sim 30 \text{ dB}$ , within the wavelength range from 1470 nm to 1580 nm. The measured polarization ER is close to the calculated value (35 dB). As it is shown in Fig. 8 (b), the TE and TM reflection coefficients are about  $-30 \text{ dB}$ . Since the reflection response of the TM mode is similar to that of the TE mode, we conclude that the reflection of the TM polarization is low, and the measured reflected power is mainly due to reflections from the chip facet. This efficient suppression of reflectivity is

an important advantage of our device compared to the previously reported SWG polarizer [16], in which the reflectivity for the blocked polarization state is large due to the Bragg effect.

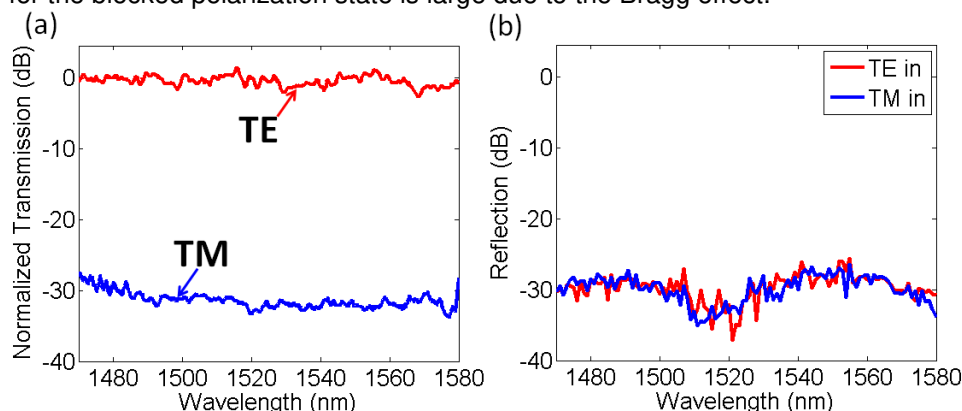


Fig. 8 Experimental characterizations of the TE-pass SWG waveguide polarizer: (a) Measured TE and TM transmission coefficients (normalized to the transmittance of the reference Si-wire waveguide). (b) Measured TE and TM reflection coefficients.

#### 4. Conclusion

We have proposed and experimentally demonstrated a low loss TE-pass polarizer based on a subwavelength grating (SWG) waveguide. Our polarizer exploits for the first time the Bloch mode cut-off condition by engineering the SWG equivalent material index. We show both by calculations and experiments that only the TE mode is supported in the SWG waveguide while the TM mode attenuates and leaks away to the silicon substrate with a low reflection. The experimental results for a device implemented in an SOI substrate with a 220 nm silicon layer yield an average TE insertion loss of 0.4 dB in a broad wavelength range 1470 nm - 1580 nm, with a remarkably high polarization extinction ratio (~30 dB). The overall device length is 60  $\mu\text{m}$ . This work paves a promising way in development of compact low-loss, low-reflectivity and fabrication tolerant silicon-based polarizing components operating over a broad wavelength range.

#### References

- [1] D. Dai, L. Liu, S. Gao, D.-X. Xu, and S. He, "Polarization management for silicon photonic integrated circuits," *Laser Photon. Rev.*, vol. 7, no. 3, pp. 303–328, May 2013.
- [2] D. Dai, Z. Wang, and J. E. Bowers, "Ultrashort broadband polarization beam splitter based on an asymmetrical directional coupler," *Opt. Lett.*, vol. 36, no. 13, pp. 2590–2592, Jul. 2011.
- [3] H. Qiu, Y. Su, P. Yu, T. Hu, J. Yang and X. Jiang, "Compact polarization splitter based on silicon grating-assisted couplers," *Opt. Lett.*, vol. 40, no. 9, pp. 1885–1887, Apr. 2015.
- [4] H. Zhang, S. Das, Y. Huang, C. Li, S. Chen, H. Zhou, M. Yu, P. Guo-Qiang Lo, and J. T. L. Thong, "Efficient and broadband polarization rotator using horizontal slot waveguide for silicon photonics," *Appl. Phys. Lett.*, vol. 101, no. 2, p. 021105, Oct. 2012.
- [5] Y. Xiong, D.-X. Xu, J. Schmid, P. Cheben, S. Janz, and W. Ye, "Robust silicon waveguide polarization rotator with an amorphous silicon overlayer," *IEEE Photonics J.*, vol. 6, no. 2, p. 2200308, Apr. 2014.
- [6] L. Chen, C. R. Doerr, and Y.-K. Chen, "Compact polarization rotator on silicon for polarization-diversified circuits," *Opt. Lett.*, vol. 36, no. 4, pp. 469–471, Feb. 2011.
- [7] A. V. Velasco, M. L. Calvo, P. Cheben, A. Ortega-Moñux, J. H. Schmid, C. A. Ramos, I. M. Fernandez, J. Lapointe, M. Vachon, S. Janz, and D.-X. Xu, "Ultracompact polarization converter with a dual subwavelength trench built in a silicon-on-insulator waveguide," *Opt. Lett.*, vol. 37, no. 3, pp. 365–367, Feb. 2012.
- [8] L. Liu, Y. Ding, K. Yvind, and J. M. Hvam, "Silicon-on-insulator polarization splitting and rotating device for polarization diversity circuits," *Opt. Express*, vol. 19, no. 13, pp.12646–12651, Jun. 2011.
- [9] H. Guan, A. Novack, M. Streshinsky, R. Shi, Q. Fang, A. E.-J. Lim, G.-Q. Lo, T. Baehr-Jones, and M. Hochberg, "CMOS-compatible highly efficient polarization splitter and rotator based on a double-etched directional coupler," *Opt. Express*, vol. 22, no. 3, pp. 2489-2496, Feb. 2014.
- [10] Y. Xiong, D.-X. Xu, J. H. Schmid, P. Cheben, S. Janz, and W. N. Ye, "Fabrication tolerant and broadband polarization splitter and rotator based on a taper-etched directional coupler," *Opt. Express*, vol. 22, no. 14, pp. 17458-17465, Jul. 2014.
- [11] M. Z. Alam, J. Stewart Aitchison, and M. Mojahedi, "Compact and silicon-on-insulator-compatible hybrid plasmonic TE-pass polarizer," *Opt. Lett.*, vol. 37, no. 1, pp. 55-57, Jan. 2012.
- [12] Y. Huang, S. Zhu, H. Zhang, T. Y. Liow, and G. Q. Lo, "CMOS compatible horizontal nanoplasmonic slot waveguides TE-pass polarizer on silicon-on-insulator platform," *Opt. Express*, vol. 21, no. 10, pp. 12790–12796, May 2013.
- [13] Y. Cui, Q. Wu, E. Schonbrun, M. Tinker, J.-B. Lee, and W. Park, "Silicon-based 2-D slab photonic crystal tm polarizer at telecommunication wavelength," *IEEE Photon. Technol. Lett.*, vol. 20, no. 8, pp. 641–643, Apr. 2008.
- [14] D. Dai, Z. Wang, N. Julian, and J. E. Bowers, "Compact broadband polarizer based on shallowly-etched silicon-on-insulator

- ridge optical waveguides," *Opt. Express*, vol. 18, no. 26, pp. 27404–27415, Dec. 2010.
- [15] Q. Wang, and S. T. Ho, "Ultracompact TM-pass silicon nanophotonic waveguide polarizer and design," *IEEE Photonics J.*, vol. 2, no. 1, pp. 49–56, Feb. 2010.
- [16] X. Guan, P. Chen, S. Chen, P. Xu, Y. Shi, and D. Dai, "Low-loss ultracompact transverse-magnetic-pass polarizer with a silicon subwavelength grating waveguide," *Opt. Lett.*, vol. 39, no. 15, pp. 4514–4517, Aug. 2014.
- [17] R. Halir, P. J. Bock, P. Cheben, A. Ortega-Moñux, C. Alonso-Ramos, J. H. Schmid, J. Lapointe, D.-X. Xu, J. G. Wangüemert-Pérez, Í. Molina-Fernández and S. Janz, "Waveguide sub-wavelength structures: a review of principles and applications," *Laser Photon. Rev.*, vol. 9, no. 1, pp. 25–49, Sep. 2014.
- [18] P. J. Bock, P. Cheben, J. H. Schmid, J. Lapointe, S. Janz, G. C. Aers, D.-X. Xu, A. Densmore, and T. J. Hall, "Subwavelength grating periodic structures in silicon-on-insulator: a new type of microphotonic waveguide," *Opt. Express*, vol. 18, no. 19, pp. 20251–20262, Sep. 2010.
- [19] P. Cheben, D.-X. Xu, S. Janz, and A. Densmore, "Subwavelength waveguide grating for mode conversion and light coupling in integrated optics," *Opt. Express*, vol. 14, no. 14, pp. 4695–4702, May 2006.
- [20] Y. Xiong, J. G. Wangüemert-Pérez, D.-X. Xu, J. H. Schmid, P. Cheben, S. Janz, and W. N. Ye, "Polarization splitter and rotator with subwavelength grating for enhanced fabrication tolerance," *Opt. Lett.*, vol. 39, no. 24, pp. 6931–6934, Dec. 2014.
- [21] P. J. Bock, P. Cheben, J. H. Schmid, J. Lapointe, A. Delâge, D.-X. Xu, S. Janz, A. Densmore, and T. J. Hall, "Subwavelength grating crossings for silicon wire waveguides," *Opt. Express*, vol. 18, no. 15, pp. 16146–16155, Jul. 2010.
- [22] J. H. Schmid, P. Cheben, P. J. Bock, R. Halir, J. Lapointe, S. Janz, A. Delâge, A. Densmore, J.-M. Fédéli, T. J. Hall, B. Lamontagne, R. Ma, Í. Molina-Fernández, and D.-X. Xu, "Refractive index engineering with subwavelength gratings in silicon microphotonic waveguides," *IEEE Photonics J.* vol. 3, no. 3, pp. 597–607, Jun. 2011.